nature immunology

ARTICLES

https://doi.org/10.1038/s41590-018-0177-0

IL-9 receptor signaling in memory B cells regulates humoral recall responses

Shogo Takatsuka[1,3], Hiroyuki Yamada[1,4], Kei Haniuda[1,4], Hiroshi Saruwatari[1], Marina Ichihashi[1], Jean-Christophe Renauld[2] and Daisuke Kitamura[1*]

Memory B cells (B_{mem} cells) are the basis of long-lasting humoral immunity. They respond to re-encountered antigens by rapidly producing specific antibodies and forming germinal centers (GCs), a recall response that has been known for decades but remains poorly understood. We found that the receptor for the cytokine IL-9 (IL-9R) was induced selectively on B_{mem} cells after primary immunization and that IL-9R-deficient mice exhibited a normal primary antibody response but impaired recall antibody responses, with attenuated population expansion and plasma-cell differentiation of B_{mem} cells. In contrast, there was augmented GC formation, possibly due to defective downregulation of the ligand for the co-stimulatory receptor ICOS on B_{mem} cells. A fraction of B_{mem} cells produced IL-9. These findings indicate that IL-9R signaling in B_{mem} cells regulates humoral recall responses.

After immunization with T cell–dependent (TD) antigens, antigen-specific B cells are activated and proliferate and can switch the isotype of B cell antigen receptors from immunoglobulin M (IgM) to IgG, IgA or IgE (class switching), with the aid of helper T cells. Some of these B cells differentiate into short-lived plasma cells (PCs) and rapidly produce antibodies, while others further proliferate to form germinal centers (GCs) in the follicles of the secondary lymphoid organs and undergo further class switching and somatic hypermutation (SHM) of their genes encoding immunoglobulin variable (V) regions. GC B cells with elevated antigen-binding affinity, as a result of SHM, are selected and differentiate into either long-lived PCs (LLPCs) or memory B cells (B_{mem} cells), both of which contribute to long-lasting humoral immunological memory. LLPCs reside mainly in the bone marrow and continue to produce high-affinity antibodies after a peak of primary antibody response, whereas B_{mem} cells remain quiescent and survive for a long period in as-yet-undefined sites. After re-encountering the same antigen that elicited the primary response, B_{mem} cells undergo a proliferative burst and then differentiate into PCs that produce high-affinity antibodies, a complex process called a 'secondary' or 'recall' response[1–3]. Thus, B_{mem} cells have a central role in acquired humoral immunity, yet the mechanisms for the generation, maintenance and recall responses of B_{mem} cells remain elusive.

In the TD immune responses, helper T cells are generally required for the formation of GCs, PCs and B_{mem} cells and for the memory recall response, working through interaction with B cells via CD40L, the ligand for the co-stimulatory receptor CD40[4–8]. However, the requirements for cytokines in these B cell reactions are not fully understood. During the immune response to protein antigens, IL-21, a signature cytokine of follicular helper T cells (T_{FH} cells), is required for IgG1 production and LLPC formation and is important but not essential for GC formation but is not necessary for B_{mem} cell development[9–14]. The requirement for IL-21 in memory recall responses to protein antigens in mice remains controversial[13–15]. IL-4 produced by T_{FH} cells has been shown to be important for IgG1 antibody responses and essential for IgE antibody responses but unnecessary for GC formation[16–18] and for the production of B_{mem} cells[13]. Signaling via the IL-2 receptor or the IL-15 receptor is not necessary for primary or secondary TD immune responses[19]. Thus, the cytokines required for the generation, maintenance and recall responses of B_{mem} cells remain unclear.

IL-9 is produced by various immune cells, such as helper T cells (exemplified by T_H9 cells), mast cells and eosinophils, as well as type 2 innate lymphoid cells (ILC2 cells), and exerts various functions depending on the target-cell types expressing its receptor (IL-9R)[20–24]. IL-9R is composed of the IL-9R α-chain and common γ-chain and is expressed on mast cells, activated T cells, ILC2 cells and basophils, among others[20,21,23,25,26]. Numerous studies have demonstrated various in vivo functions of IL-9, including the promotion of allergic and autoimmune diseases, protection from parasite infection and inhibition of tumor growth[21,27]. As for B cells, it has been reported that IL-9 potentiates the IL-4-induced production of IgE and IgG in vitro[28,29] and in vivo expansion of the peritoneal B-1 cell subset[30]. However, the role of IL-9 signaling in the aforementioned TD immune response remains unknown.

Here we found that IL-9R was selectively expressed on B_{mem} cells and that the population expansion and antibody production of B_{mem} cells after secondary immunization was markedly attenuated in IL-9R-deficient mice due to a B cell–intrinsic defect. Notably, IL-9 was produced by a fraction of B_{mem} cells in the secondary response. Thus, we propose a novel regulatory mechanism for the humoral recall response via autocrine and/or paracrine IL-9–IL-9R signaling by B_{mem} cells.

Results

Expression of IL-9R on B_{mem} cells. To understand how B_{mem} cells are regulated, we analyzed the gene-expression profiles of induced memory-like B cells (iMB cells) as a surrogate for B_{mem} cells[31], compared with those of naive follicular B cells. Among genes encoding cell-surface molecules 'preferentially' expressed

[1]Division of Molecular Biology, Research Institute for Biomedical Sciences (RIBS), Tokyo University of Science, Noda, Japan. [2]Ludwig Institute for Cancer Research and Experimental Medicine Unit, Universite catholique de Louvain, Brussels, Belgium. [3]Present address: Department of Chemotherapy and Mycoses, National Institute of Infectious Diseases, Tokyo, Japan. [4]These authors contributed equally: Hiroyuki Yamada, Kei Haniuda.
*e-mail: kitamura@rs.noda.tus.ac.jp

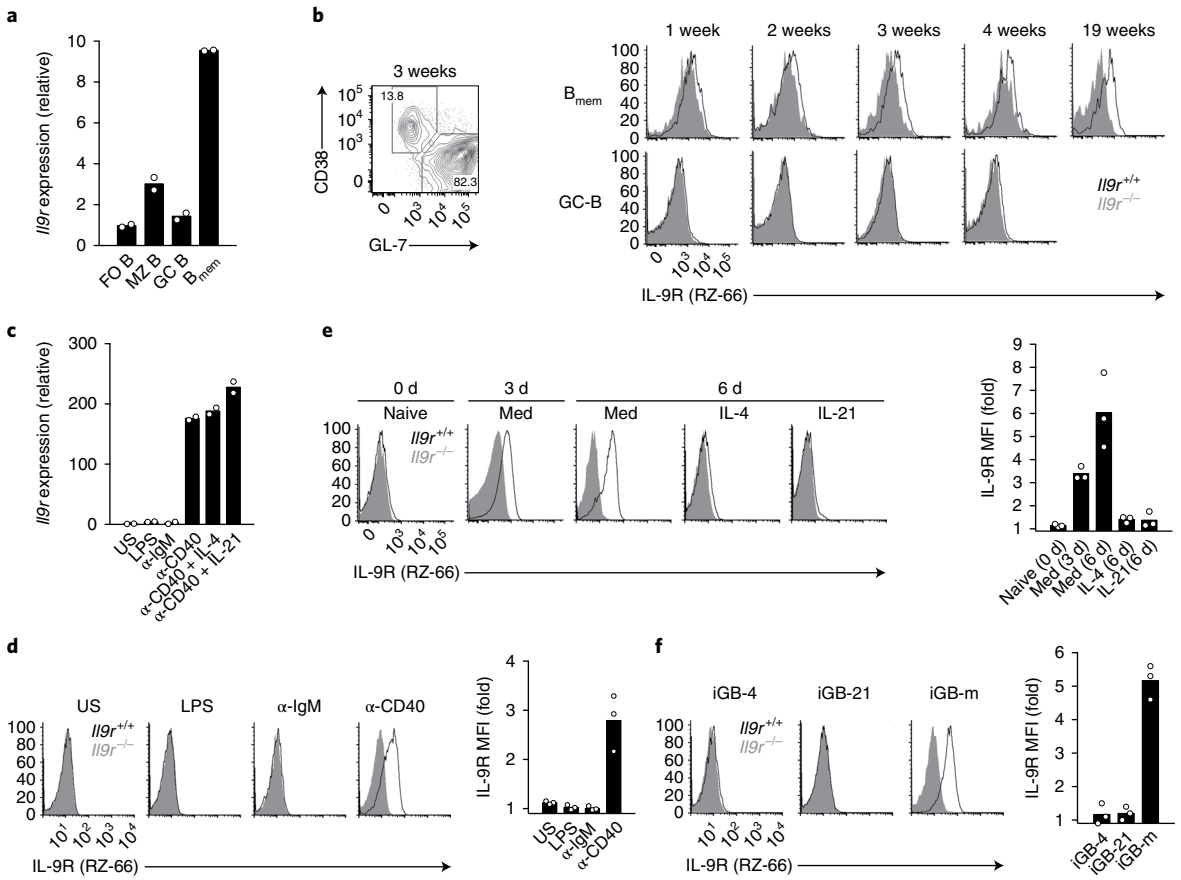

Fig. 1 | Expression of IL-9R on B cells. a, qRT-PCR analysis of *Il9r* mRNA in follicular B cells (FO B), marginal zone B cells (MZ B), GC B cells (GC B) and B_{mem} cells (B_{mem}) sorted from C57BL/6 mice; results were normalized to those of the control gene *Gapdh*. **b**, Flow-cytometry analysis of IL-9R expression (right) on B_{mem} cells and GC B cells (left margin; gating, left) sorted from the spleen of *Il9r*$^{+/+}$ or *Il9r*$^{-/-}$ mice (key) immunized with NP-CGG in alum 1 week or 2, 3, 4 or 19 weeks earlier (above plots), assessed by staining with monoclonal antibody RZ-66 to mouse IL-9R. Numbers in outlined areas (left plot) indicate percent CD38^{hi}GL-7^{-} (B_{mem}) cells (top left) or CD38^{lo}GL-7^{+} (GC B) cells (bottom right) among B220^{+}IgG1^{+}NP^{+} cells. **c**, qRT-PCR analysis of *Il9r* mRNA in splenic naive B cells obtained from C57BL/6 mice and left unstimulated (US) or stimulated for 72 h with lipopolysaccharide (LPS), anti-IgM (α-IgM), anti-CD40 (α-CD40), or α-CD40 plus IL-4 or IL-21 (horizontal axis); results presented as in **a**. **d**–**f**, Flow-cytometry analysis (left) of IL-9R expression (via RZ-66) on *Il9r*$^{+/+}$ or *Il9r*$^{-/-}$ splenic naive B cells (key) left unstimulated or stimulated as in **c** (**d**), cultured on 40LB feeder cells for 0 d (Naive) or for 3 or 6 d (above plots) with medium alone (Med) or with IL-4 or IL-21 (above plots) (**e**), or cultured on 40LB feeder cells for 3 d with IL-4 (iGB-4), then 3 d with IL-21 (iGB-21), and further 3 d with medium alone (iGB-m), with iGB-21 and iGB-m cells gated as IgG1^{+} CD138^{-} (**f**); right, mean fluorescent intensity (MFI) of IL-9R in cells as at left (horizontal axis), presented as the ratio of the results for *Il9r*$^{+/+}$ cells to those for *Il9r*$^{-/-}$ cells (fold values). Each symbol (**a**,**c**–**f**) represents an individual replicate (**a**,**c**) or mouse (**d**–**f**); bar top, mean of group. Data are representative of two independent experiments with similar results (**a**,**c**), with $n = 2$ technical replicates of one biological sample per group (**a**) or per experiment (**c**); one experiment to three independent experiments with similar results (**b**; Supplementary Fig. 1b); or three independent experiments with $n = 1$ mouse per genotype in each (**d**–**f**)

in iMB cells, we focused on *Il9r*. Quantitative RT-PCR analysis revealed that *Il9r* transcripts were more abundant in B_{mem} cells than in naive follicular B cells, marginal-zone B cells or GC B cells (Fig. 1a).

To detect IL-9R protein on the cell surface, we generated a panel of monoclonal antibodies to IL-9R (Supplementary Fig. 1a). Using one of those antibodies, we analyzed by flow cytometry ex vivo spleen cells from wild-type C57BL/6 mice, and from *Il9r*$^{-/-}$ mice[32] (as a negative control), immunized with a conjugate of the hapten NP and chicken γ-globulin (CGG) in aluminum hydroxide (alum), or not immunized. IL-9R protein was expressed on the surface of B_{mem} cells from 1 week after immunization onward, whereas it was much less abundant on the surface of GC B cells (Fig. 1b and Supplementary Fig. 1b). As has been reported[33], GC-derived memory precursor cells (GC-MPs; defined as CD38^{+}GL-7^{+}Fas^{+}) also expressed IL-9R, albeit less abundantly than B_{mem} cells did (Supplementary Fig. 1c). IL-9R was also detectable on mast cells and a small fraction of basophils and plasmacytoid dendritic cells, but it was barely expressed on other lineages of hematopoietic cells from the spleen of immunized mice (Supplementary Fig. 1d) and mice that were not immunized (data not shown).

In vitro stimulation of naive B cells with an agonistic CD40-specific antibody, to mimic interaction with CD40L, substantially upregulated the expression of *Il9r* mRNA and of IL-9R protein on the cell surface, but such upregulation was not observed after stimulation with lipopolysaccharide or antibody to IgM (anti-IgM) (Fig. 1c,d and Supplementary Fig. 1e). IL-9R expression was also induced when naive B cells were cultured for 3 d on feeder cells expressing CD40L and the pro-survival cytokine BAFF (40LB cells) and was further upregulated during the next 3 d on the same feeder cells in standard culture medium. In contrast, inclusion of IL-4 or IL-21 in the culture medium suppressed the IL-9R expression in the subsequent 3-day culture period (Fig. 1e). When naive B cells were cultured on 40LB feeder cells, initially with IL-4 and subsequently with IL-21 (collectively called

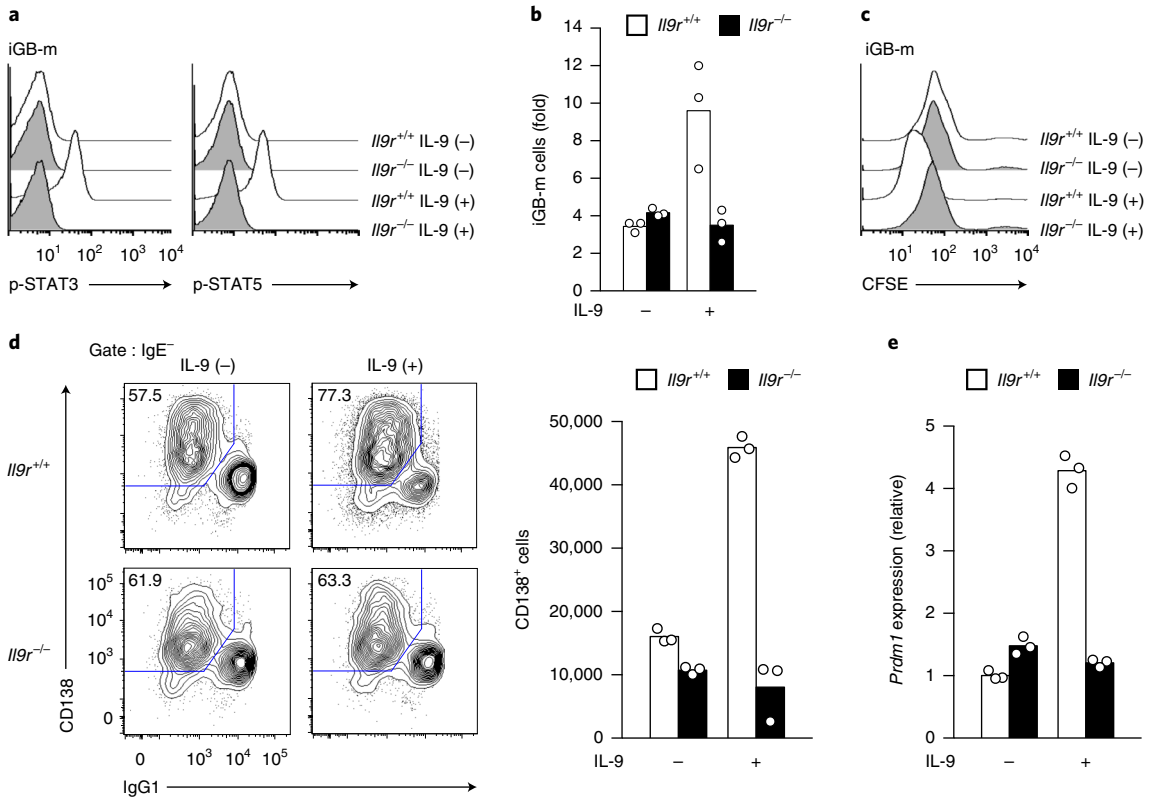

Fig. 2 | Function of IL-9R on B cells in vitro. a, Flow-cytometry analysis of phosphorylated (p-) STAT3 and STAT5 in *Il9r*$^{+/+}$ or *Il9r*$^{-/-}$ iGB-m cells at day 9 after culture for 10 min with (+) or without (–) IL-9 (right margin). **b**, Quantification of live *Il9r*$^{+/+}$ or *Il9r*$^{-/-}$ iGB-m cells (key) cultured with or without IL-9 (horizontal axis) from day 6 to day 9, presented as the ratio of the number of cells on day 9 to that on day 6 ('fold' values). **c**, Flow-cytometry analysis of the CFSE fluorescence of cells cultured as in **b** (right margin) and labeled on day 6, assessed on day 9. **d**, Flow cytometry (left) of *Il9r*$^{+/+}$ or *Il9r*$^{-/-}$ iGB-m cells (left margin) cultured for 2 d as in **b** (above plots); right, quantification of CD138$^+$ PCs in those cultures. Numbers in outlined areas (left) indicate percent CD138$^+$IgG1$^+$ PCs. **e**, qRT-PCR analysis of *Prdm1* mRNA in IgE$^-$CD138$^-$ iGB-m cells cultured as in **d**; results normalized to those of *Gapdh*. Each symbol (**b**,**d**,**e**) represents an individual replicate; bar top, mean of group. Data are representative of three (**a**–**d**) or two (**e**) independent experiments with similar results, with $n = 3$ technical replicates per group of one biological sample per genotype (**b**,**d**,**e**)

'iGB cell cultures')[31], cell-surface expression of IL-9R was not detected. However, IL-9R expression was induced on the cells after a tertiary culture without cytokines ('iGB-m cells') (Fig. 1f and Supplementary Fig. 1f). Notably, the IL-4- or IL-21-mediated suppression of IL-9R expression was not at the level of RNA, as assessed by RT-PCR (Fig. 1c). These data indicated that IL-9R expression on B cells was induced by stimulation with CD40 but was suppressed by simultaneous stimulation with IL-4 or IL-21, which might have accounted for the low IL-9R expression on GC B cells in vivo.

IL-9 promotes B cell proliferation and differentiation. Using iGB-m cells expressing IL-9R on their surface, we assessed the function of IL-9R signaling in B cells. We cultured those iGB-m cells, as well as iGB-m cells from *Il9r*$^{-/-}$ mice, as a negative control, on the 40LB feeder cells and treated the cultures with IL-9. First, we demonstrated that the IL-9R on iGB-m cells was functional, since treatment with IL-9 induced phosphorylation of the transcription factors STAT3 and STAT5 only in IL-9R-sufficient cells (Fig. 2a), similar to a published report on human tonsillar B cells[34]. Treatment with IL-9 facilitated the proliferation of IL-9R-sufficient iGB-m cells, as demonstrated by the increase in cell number (Fig. 2b) and dilution of the cell-division-tracking dye CFSE in B cells (Fig. 2c). IL-9 also augmented differentiation of the iGB-m cells into PCs (Fig. 2d) and expression of *Prdm1* mRNA (which encodes the transcriptional repressor Blimp-1) (Fig. 2e) via IL-9R.

IL-9R signaling facilitates the antibody recall response. To address the role of IL-9R expressed on B cells in vivo, we analyzed the TD immune responses of *Il9r*$^{-/-}$ and *Il9r*$^{+/+}$ mice. Mice were first immunized intraperitoneally (i.p.) with NP-CGG in alum and were boosted with soluble NP-CGG intravenously (i.v.) 6 weeks later, and the concentration of NP-specific antibodies in serum was measured periodically after the primary immunization. The IgG1 response in *Il9r*$^{-/-}$ mice was similar to that in *Il9r*$^{+/+}$ mice, as measured from 1 week to 6 weeks after the primary immunization, but the secondary IgG1 response, as measured until 3 weeks after the booster immunization, was markedly attenuated in *Il9r*$^{-/-}$ mice (Fig. 3a). The secondary responses of IgM and other IgG subclasses were assessed in serum obtained 2 weeks after the booster immunization. The titers of IgM, IgG2c and IgG3 were too low to be reliably evaluated. The titer of IgG2b was clearly measurable and was found to be attenuated in *Il9r*$^{-/-}$ mice (Supplementary Fig. 2a). To test the generality of these findings, we used another, more physiological immunization with a vaccine containing whole inactivated influenza virus. As a result of this immunization, the secondary IgG response to the hemagglutinin epitope was significantly suppressed in *Il9r*$^{-/-}$ mice (Fig. 3b), while the primary IgG response to the same epitope assessed at 3 weeks after the primary immunization was unaffected (data not shown). A similar attenuation of the NP-specific antibody recall response was observed in mixed–bone marrow chimeras generated by the transfer of a mixture of bone marrow cells from *Il9r*$^{+/+}$ or *Il9r*$^{-/-}$ mice and μMT mice (which lack mature B cells) into

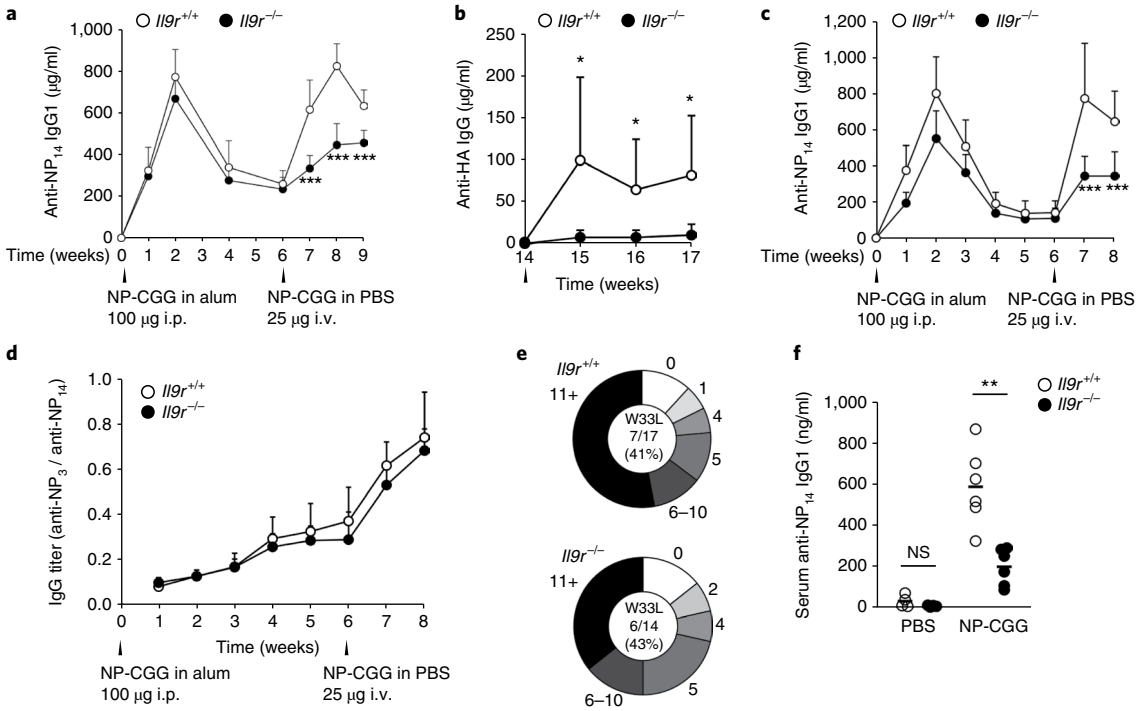

Fig. 3 | Attenuated recall antibody responses to TD antigen in *Il9r*$^{-/-}$ mice. a, ELISA of anti-NP_{14} IgG1 in serum from *Il9r*$^{+/+}$ or *Il9r*$^{-/-}$ mice (key; $n=7$ per genotype) immunized i.p. with NP-CGG in alum and boosted i.v. with soluble NP-CGG (in PBS) 45 d later (below plot; upward arrowheads), assessed at various times (horizontal axis) after the initial immunization. **b**, ELISA of IgG antibody to hemagglutinin (Anti-HA IgG) in serum from *Il9r*$^{+/+}$ mice ($n=8$) or *Il9r*$^{-/-}$ mice ($n=7$) (key) at various times (horizontal axis) after secondary immunization i.v. with formalin-inactivated whole influenza A virus, subtype H1N1, strain A/Puerto Rico/8/34 (upward arrowhead), given at 14 weeks after primary immunization subcutaneously with the same antigen (inactivated virus). **c**, ELISA of anti-NP_{14} IgG1 in serum from mixed-bone marrow chimeras ($n=10$) reconstituted with *Il9r*$^{+/+}$ or *Il9r*$^{-/-}$ B cells (key) and immunized as in **a**. **d**, Quantification of anti-NP IgG1 in mice as in **c**, presented as the ratio of anti-NP_3 to anti-NP_{14}. **e**, SHM of V_H186.2-encoding genes in pooled NP^+IgG1^+ B_{mem} cells from *Il9r*$^{+/+}$ or *Il9r*$^{-/-}$ mice ($n=6$ per genotype; top left of each plot) at 10 weeks after intraperitoneal immunization with NP-CGG in alum, presented as the frequency ('pie slices') of V_H186.2-encoding sequences with various numbers of mutations (along perimeter; '11+' indicates 11 or more), and the ratio and frequency (in parenthesis) of the sequence encoding the W33L substitution (center). **f**, ELISA of anti-NP_{14} IgG1 in serum from wild-type C57BL/6 mice given adoptive transfer of *Il9r*$^{+/+}$ or *Il9r*$^{-/-}$ B_{mem} cells (key) and spleen cells from CGG-primed *Il9r*$^{+/+}$ mice 1 d before intravenous injection of soluble NP-CGG ($n=6$ host mice) or PBS ($n=4$ host mice), assessed 7 d later. Each symbol represents an individual mouse; small horizontal lines indicate the mean. NS, not significant ($P>0.05$); $^*P<0.05$, $^{**}P<0.01$ and $^{***}P<0.001$ (two-tailed unpaired Student's *t*-test). Data are representative of two (**a**–**d**,**f**) or three (**e**) independent experiments with similar results (mean + s.d. in **a**–**d**)

irradiated wild-type C57BL/6 mice (Fig. 3c); this indicated that IL-9R on B cells was required for a normal recall response.

During the entire TD immune response, the affinity maturation of serum antibodies in *Il9r*$^{-/-}$ was not significantly different from that in *Il9r*$^{+/+}$ mice, as assessed by the titer of IgG1 that bound to NP epitopes of low valency, relative to the total IgG1 titer (Fig. 3d). The frequency of overall mutations and the mutation encoding the W33L substitution (indicative of an increase in affinity for NP)[35] in gene sequences encoding the heavy-chain variable region V_H186.2 of NP-specific $IgG1^+$ B_{mem} cells in *Il9r*$^{-/-}$ mice was similar to that in *Il9r*$^{+/+}$ mice at 10 weeks (Figs. 3e) and 2 weeks (Supplementary Fig. 2b) after primary immunization. These data indicated that the 'gross affinity' of B_{mem} cells for antigen increased normally in *Il9r*$^{-/-}$ mice despite their defective antibody recall response.

To assess more directly the ability of IL-9R-deficient B_{mem} cells to produce antibody in response to secondary immunization, we transferred the same number of NP-specific $IgG1^+$ B_{mem} cells from NP-primed *Il9r*$^{-/-}$ or *Il9r*$^{+/+}$ mice into recipient mice, together with carrier-primed spleen cells, and immunized the recipient mice with soluble NP–carrier conjugates. Measurement of serum titers demonstrated that the mice given transfer of *Il9r*$^{-/-}$ B_{mem} cells produced about threefold less anti-NP IgG1, on average, than did mice that received *Il9r*$^{+/+}$ B_{mem} cells (Fig. 3f).

Collectively, these findings indicated that IL-9R on B_{mem} cells were required for a normal recall antibody response in mice.

The formation and maintenance of B_{mem} cells in *Il9r*$^{-/-}$ mice. To elucidate the cause of the defective recall response in *Il9r*$^{-/-}$ mice, we analyzed spleen cells from *Il9r*$^{-/-}$ and *Il9r*$^{+/+}$ mice by flow cytometry after primary immunization of the mice with NP-CGG. The number of $IgG1^+$ NP-binding (NP^+) GC B cells was slightly but not significantly lower, on average, in *Il9r*$^{-/-}$ mice than in *Il9r*$^{+/+}$ mice at 2 weeks after immunization (Fig. 4a and Supplementary Fig. 3a). Similarly, no significant difference was observed in the number of $IgG1^+$ NP^+ B_{mem} cells in *Il9r*$^{-/-}$ mice and that in *Il9r*$^{+/+}$ mice at 4 or 10 weeks after immunization (Fig. 4b,c and Supplementary Fig. 3b) or in the number of such cells in mixed–bone marrow chimeras (generated as for Fig. 3c) given *Il9r*$^{-/-}$ cells and those given *Il9r*$^{+/+}$ cells, assessed at 12 weeks after immunization (Supplementary Fig. 3c). Very few non–IgG1 class-switched B_{mem} cells were present in the immunized mice, but no significant differences between *Il9r*$^{-/-}$ mice and *Il9r*$^{+/+}$ mice were observed (Fig. 4b and Supplementary Fig. 3b). To determine if IgM^+ B_{mem} cells were affected by the lack of IL-9R, we obtained naive B cells from *Il9r*$^{-/-}$ and *Il9r*$^{+/+}$ $CD45.1^+$ mice carrying a knock-in allele encoding an NP-specific V_H region (B1-8ki), labeled the cells with CFSE and transferred them into wild-type C56BL/6 host

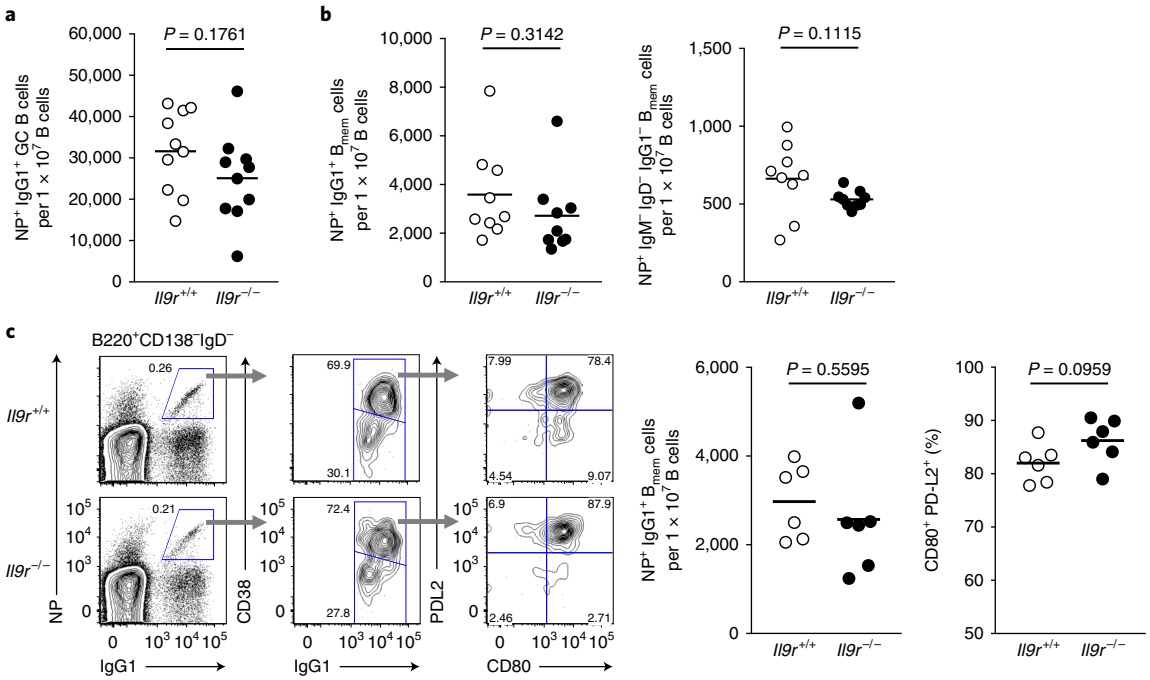

Fig. 4 | The formation and maintenance of B_{mem} cells in the primary TD response. a,**b**, Quantification of NP+ IgG1+ GC B cells (**a**; gating, Supplementary Fig. 3a) or NP+ IgG1+ (**b**, left) or NP+ IgM−IgD−IgG1− (**b**, right) B_{mem} cells (**b**; gating, Supplementary Fig. 3b) in the spleen of *Il9r*$^{+/+}$ or *Il9r*$^{-/-}$ mice (horizonal axis; $n=10$ (**a**) or $n=9$ (**b**) per genotype) immunized i.p. with NP-CGG in alum 2 weeks (**a**) or 4 weeks (**b**) previously. **c**, Quantification of NP+ IgG1+ B_{mem} cells in the spleen (middle right) and frequency of CD80+PD-L2+ cells among the B_{mem} cells (far right) in *Il9r*$^{+/+}$ and *Il9r*$^{-/-}$ mice (horizonal axis; $n=6$ per genotype) immunized i.p. with NP-CGG in alum 10 weeks earlier; left, gating of cells assessed at right. Numbers in outlined areas or quadrants (left) indicate percent cells in each. Each symbol represents an individual mouse; small horizontal lines indicate the mean. *P* values, two-tailed unpaired Student *t*-test. Data are pooled from five independent experiments (**a**) or are representative of two independent experiments with similar results (**b**,**c**)

mice, which we then immunized with NP-CGG. 24 d later, B_{mem} cells were detected as donor-derived CFSE^{lo} (fully divided) NP+ CD38+ B cells[36], although the number of IgM+ B_{mem} cells as well as IgG1+ B_{mem} cells in recipients of *Il9r*$^{-/-}$ B cells did not significantly differ from that in recipients of *Il9r*$^{+/+}$ B cells (Supplementary Fig. 3d). Also, no significant difference between *Il9r*$^{-/-}$ mice and *Il9r*$^{+/+}$ mice was observed in the proportion of the CD80+ PD-L2+ IgG1+B_{mem} cell subpopulation that is proposed to be prone to differentiate into PCs after the secondary immunization[37] (Fig. 4c) or in the number of CD80+ PD-L2+ CD73+ IgG1+ B_{mem} cells that have also been identified as being prone to differentiate into PCs[38,39] (Supplementary Fig. 3e). These data indicated that the formation and maintenance of long-lived B_{mem} cells and their subpopulations were largely normal in the absence of IL-9R during the primary response and thus this could not be the main reason for the defective antibody recall response in *Il9r*$^{-/-}$mice.

Abnormal response of IL-9R-deficient B_{mem} cells. To analyze the defect of the recall response in *Il9r*$^{-/-}$ mice at a cellular level, we compared the number of NP+ IgG1+ B_{mem} cells estimated by flow cytometry at 3.5 d after secondary immunization with that after mock immunization (with PBS) (Fig. 5a). The proliferative expansion of B_{mem} cells in the immunized mice relative to that in mock-immunized mice was significantly lower in *Il9r*$^{-/-}$ mice than in *Il9r*$^{+/+}$ mice (Fig. 5a). A similar attenuation in the proliferation of *Il9r*$^{-/-}$ B_{mem} cells after secondary immunization was observed in mixed–bone marrow chimeras reconstituted with a mixture of μMT and *Il9r*$^{-/-}$ bone marrow (Supplementary Fig. 4a). In addition, the generation of antigen-specific IgG1+ PCs was markedly attenuated in *Il9r*$^{-/-}$ mice, as was evident at 5 d after secondary immunization (Fig. 5b).

We then assessed the effect of IL-9 on B_{mem} cells in vitro. We sorted NP-binding IgG1+ B_{mem} cells from *Il9r*$^{+/+}$ and *Il9r*$^{-/-}$ mice immunized with NP-CGG in alum 10 weeks earlier and cultured them on 40LB feeder cells with or without IL-9. The proliferation of B_{mem} cells from *Il9r*$^{+/+}$ mice was clearly augmented by IL-9, but that of such cells from *Il9r*$^{-/-}$ mice was not (Fig. 5c). In addition, IL-9 induced *Il9r*$^{+/+}$ B_{mem} cells to differentiate into PCs (Fig. 5d) and produce antibodies (Fig. 5e), whereas B_{mem} cells from *Il9r*$^{-/-}$ mice failed to do so. IL-9 did not affect the survival of B_{mem} cells or that of GC B cells and naive B cells during culture without feeder cells (Supplementary Fig. 4b). These data indicated that the attenuated antibody recall response in *Il9r*$^{-/-}$ mice was due to defects in the early proliferation of B_{mem} cells and their differentiation into PCs.

Despite the attenuated proliferation of B_{mem} cells in the early phase of the recall response, the generation of antigen-specific IgG1+ GC B cells was augmented in *Il9r*$^{-/-}$ mice, as was evident at 7 d after secondary immunization (Fig. 6a). Since GC formation after secondary challenge is dependent on the co-stimulatory receptor ICOS and its ligand (ICOSL)[40,41], we assessed the expression of ICOSL on B cells. ICOSL was expressed on the iGB-m cells, as on naive B cells[42,43], but its expression was downregulated by treatment with IL-9 in an IL-9R-dependent manner, at the level of protein as well as mRNA (Fig. 6b,c). The surface expression of other molecules involved in GC formation, such as major histocompatibility complex class II, CD80, CD40 and IL-21R, was unaffected by the IL-9 signaling (Supplementary Fig. 5a). ICOSL expression was also downregulated by IL-9 in ex vivo B_{mem} cells from *Il9r*$^{+/+}$ mice, but not in those from *Il9r*$^{-/-}$ mice (Fig. 6d). Finally, administration of suboptimal dose of an ICOSL-blocking antibody just before and after the secondary immunization with NP-CGG reduced the number of responding IgG1+ GC B cells in *Il9r*$^{-/-}$ mice to a level similar to that

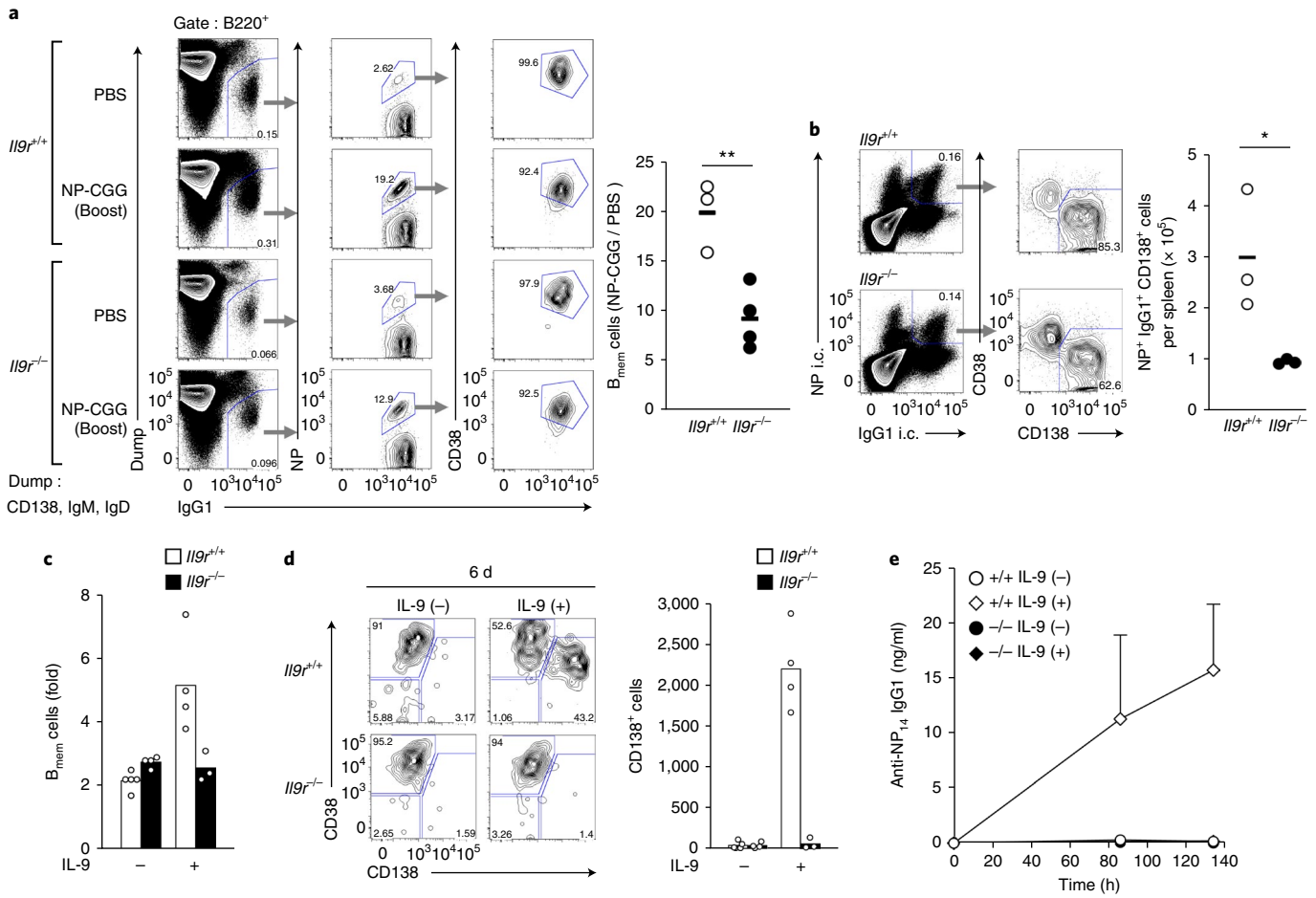

Fig. 5 | Attenuated population expansion and differentiation of *Il9r*$^{-/-}$ B_{mem} cells during a recall response. a,**b**, Flow cytometry (left) showing the gating of spleen cells from *Il9r*$^{+/+}$ or *Il9r*$^{-/-}$ mice immunized i.p. with NP-CGG in alum 12 weeks (**a**) or 20 weeks (**b**) previously and re-challenged i.p. with soluble NP-CGG (boost) or PBS 3.5 d previously (**a**) or with NP-CGG 5 d previously (**b**) (left margin); right, quantification of B_{mem} cells, presented as the ratio of the calculated number of B_{mem} cells in each 'boosted' mouse to the average number of those cells in mice given injection of PBS (NP-CGG/PBS) (**a**), or quantification of PCs producing NP-binding IgG1, per spleen (**b**), from such *Il9r*$^{+/+}$ mice ($n=3$) or *Il9r*$^{-/-}$ mice ($n=4$ (**a**) or $n=3$ (**b**)). i.c., intracellular. Numbers in outlined areas (left) indicate percent cells in each. Each symbol (right) represents an individual mouse; small horizontal lines indicate the mean. **c**, Quantification of live NP$^+$ IgG1$^+$ B_{mem} cells obtained from *Il9r*$^{+/+}$ and *Il9r*$^{-/-}$ mice (key) 10 weeks after intraperitoneal immunization with NP-CGG in alum and then cultured for 6 d on a 40LB feeder layer (1×10^3 cells per well) with or without IL-9 (horizontal axis); results presented as the ratio of the number of cells on day 6 to that on day 0 ('fold' values). **d**, Flow cytometry (left) of B_{mem} cells after culture as in **c**, showing gating strategy; right, quantification of CD138$^+$ PCs among those cells. Numbers in outlined areas (left) indicate percent cells in each. **e**, ELISA of anti-NP IgG1 in supernatants of B_{mem} cells cultured for 86 h or 134 h (horizontal axis) as in **c** (key). $^*P<0.05$ and $^{**}P<0.01$ (two-tailed unpaired Student's *t*-test, **a**,**b**). Each symbol (**c**,**d**) represents an individual replicate; bar tops indicate the mean of $n=5$ (*Il9r*$^{+/+}$, – IL-9), $n=4$ (*Il9r*$^{-/-}$, – IL-9), $n=4$ (*Il9r*$^{+/+}$, + IL-9) or $n=3$ (*Il9r*$^{-/-}$, + IL-9) technical replicates per group of samples pooled from $n=20$ mice per genotype. Data are representative of two independent experiments with similar results (mean + s.d. in **e** of replicates as in **c**,**d**)

in *Il9r*$^{+/+}$ mice (Fig. 6e and Supplementary Fig. 5b). Thus, the augmented generation of GCs in *Il9r*$^{-/-}$ mice during the recall response was probably due to a defect in the IL-9R-mediated downregulation of ICOSL on B_{mem} cells. Collectively, these results indicated that IL-9 facilitated B_{mem} cells to proliferate and then differentiate to PCs while hampering their GC formation and thus augmented the recall antibody production in mice.

B_{mem} cells produce IL-9. It has been reported that IL-9 is produced by T_H9 cells or other cells such as mast cells and ILC2 cells[20–24]. It has also been reported that a small fraction of T_{FH} cells produce IL-9 at 1 week after primary immunization[33], a result we also observed, albeit in an even smaller fraction (Supplementary Fig. 6a,b). In order to clarify whether memory helper T cells were the source of IL-9 during the recall response, we transferred naive ovalbumin (OVA)-specific CD4$^+$ T cells from OT-II mice (which have transgenic expression of an OVA-specific T cell antigen receptor) into C57BL/6 mice, which we then immunized with NP-conjugated OVA (NP-OVA) in alum (procedure, Supplementary Fig. 6c). Then, 23 weeks later, we re-challenged the same mice with soluble NP-OVA and analyzed spleen cells ex vivo 3 d later. These spleen cells produced IL-9 after in vitro culture without any particular stimulation (Fig. 7a). We then analyzed these spleen cells by flow cytometry. The donor-derived OT-II T cells exhibited memory T_{FH} cell phenotype (CD62L$^+$CXCR5$^+$)[5] and had undergone population expansion after the re-challenge (Supplementary Fig. 6d,e), but these cells were negative for IL-9 expression (Fig. 7b,d). Instead, IL-9-expressing cells were found among NP$^+$ IgG1$^+$ B_{mem} cells in the same mice (Fig. 7c,d). That finding was confirmed by the immunization (with NP-CGG) of mice without cell transfer: similar to the results noted above, a significant

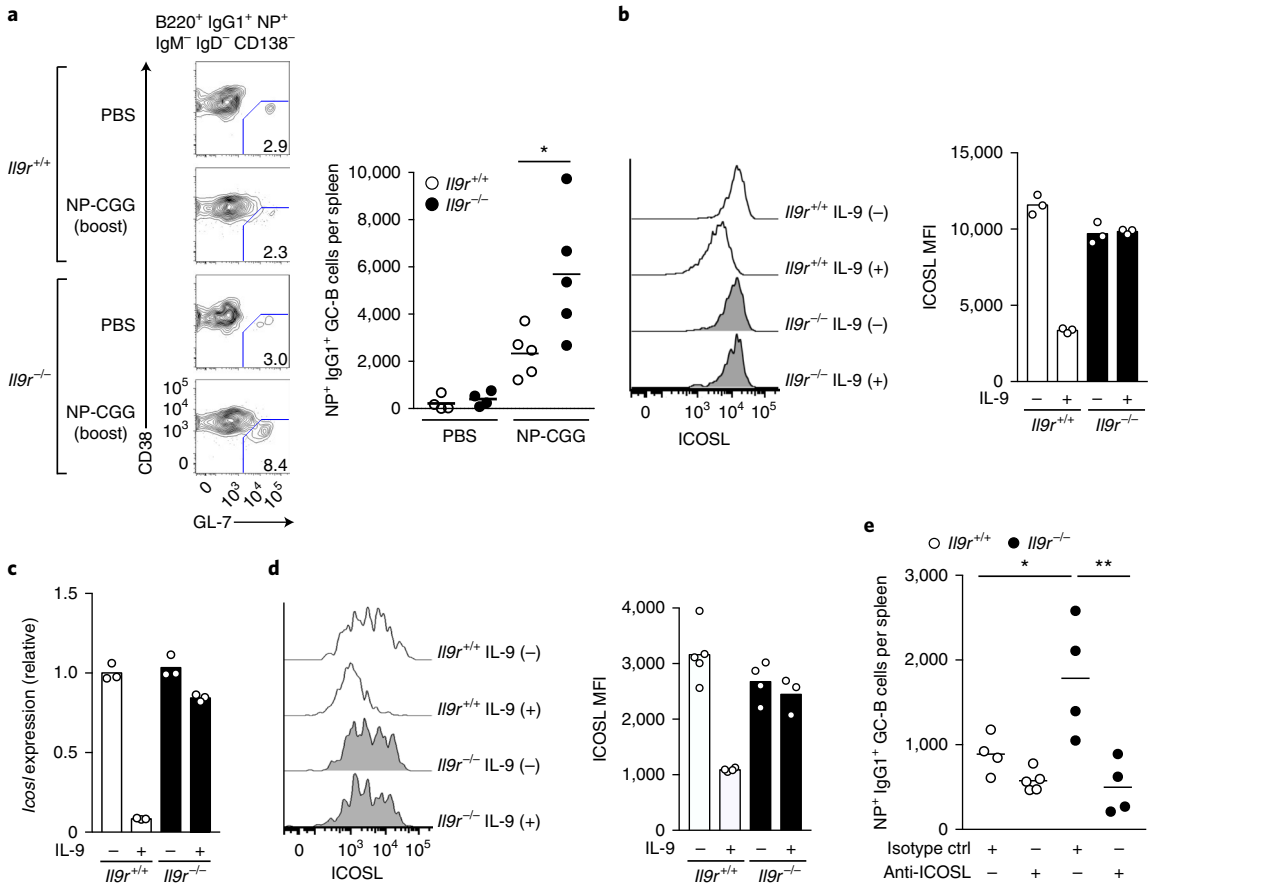

Fig. 6 | Augmented formation of GC B cells by *Il9r*$^{-/-}$ B_{mem} cells during a recall response. a, Flow cytometry (left) showing the gating of spleen cells from *Il9r*$^{+/+}$ and *Il9r*$^{-/-}$ mice (far left margin) immunized i.p. with NP-CGG in alum and, 18 weeks later, given injection of soluble NP-CGG (boost) or PBS (left margin) and assessed 7 d later; right, quantification of IgG1$^+$ GC B cells per spleen in such mice ($n = 5$ (soluble NP-CGG) or $n = 4$ (PBS) per genotype). Numbers in outlined areas (left) indicate percent CD38$^-$GL-7$^+$ cells. **b**, Flow-cytometry analysis (left) of ICOSL expression on IgE$^-$CD138$^-$ iGB-m cells after tertiary culture for 3 d with or without IL-9 (right margin); right, MFI of ICOSL in cells as at left (below plot). **c**, qRT-PCR analysis of *Icosl* mRNA in IgE$^-$CD138$^-$ iGB-m cells after culture for 2 d as in **b**; results normalized to those of *Gapdh*. **d**, Flow-cytometry analysis (left) of ICOSL expression on B_{mem} cells cultured for 6 d on 40LB feeder layer with or without IL-9; right, MFI of ICOSL on such cells (below plot). **e**, Quantification of IgG1$^+$ GC B cells per spleen of mice immunized i.p. with NP-CGG in alum and, 28 weeks later, with soluble NP-CGG under ICOSL-blocking conditions (Anti-ICOSL+) or in the presence of an isotype-matched control antibody (Isotype ctrl+) and assessed 7 d later. Each symbol represents an individual mouse (**a**,**e**) or replicate (**b**–**d**); small horizontal lines indicate the mean of the group (**a**,**e**), and bar tops indicate the mean of $n = 3$ technical replicates per group of one biological sample per genotype (**b**,**c**) or of $n = 5$ (*Il9r*$^{+/+}$, – IL-9), $n = 4$ (*Il9r*$^{+/+}$, + IL-9; *Il9r*$^{-/-}$, – IL-9) or $n = 3$ (*Il9r*$^{-/-}$, + IL-9) technical replicates of samples pooled from $n = 20$ mice per genotype (**d**). $^*P < 0.05$ and $^{**}P < 0.01$ (two-tailed unpaired Student's *t*-test (**a**) or two-way analysis of variance (**e**)). Data are representative of two (**a**,**c**,**d**) or three (**b**) independent experiments with similar results

fraction of NP$^+$ IgG1$^+$ B_{mem} cells were IL-9$^+$ at 3.5 d after the secondary immunization (Fig. 7e). Kinetic analysis after the secondary immunization demonstrated that the frequency of the IL-9-expressing B_{mem} cells in these mice increased from day 2 and peaked around day 3, reaching about 15–20% of NP$^+$ IgG1$^+$ B_{mem} cells (Fig. 7f). A small proportion of B_{mem} cells expressed IL-9 even before the secondary immunization in these mice, and these cells emerged by 2 weeks after the primary immunization (Supplementary Fig. 7a,b). Accordingly, we were able to detect IL-9 secreted from ex vivo B_{mem} cells after they were cultured on 40LB feeder cells (Supplementary Fig. 7c). Notably, neither CD38^{lo} GC B cells (Supplementary Fig. 7a,b) nor IgM$^+$ B_{mem} cells (Supplementary Fig. 7d) in the primary response produced appreciable amounts of IL-9. These data showed that a fraction of B_{mem} cells produced IL-9, with an increasing proportion doing so during the recall response.

Discussion

The memory response is a core feature of acquired immunity; however, the mechanisms that regulate the recall response of B_{mem} cells have remained obscure. As demonstrated here, we found that IL-9R was selectively expressed on B_{mem} cells during a TD immune response and that signaling through IL-9R on B_{mem} cells positively regulated their early population expansion and antibody production. Additionally, IL-9R negatively regulated GC formation during the recall response, possibly by signaling downregulation of ICOSL expression. We also found that a sizable fraction of B_{mem} cells produced IL-9 that probably stimulated even more B_{mem} cells in an autocrine or paracrine manner during the recall response. Thus, we have identified IL-9–IL-9R signaling as a direct regulator of the B_{mem} cell recall response.

We observed that surface expression of IL-9R was induced on B cells in vitro by stimulation through CD40, while it was suppressed, in a reversible manner, by concomitant stimulation with IL-4 or IL-21. Although we do not yet know the mechanism or the meaning of this cytokine-mediated suppression of IL-9R expression, it might account for our observation that GC B cells in vivo had very low expression of IL-9R. Thus, IL-4 and IL-21 produced by T_{FH} cells in the GC probably suppress IL-9R expression by neighboring GC B

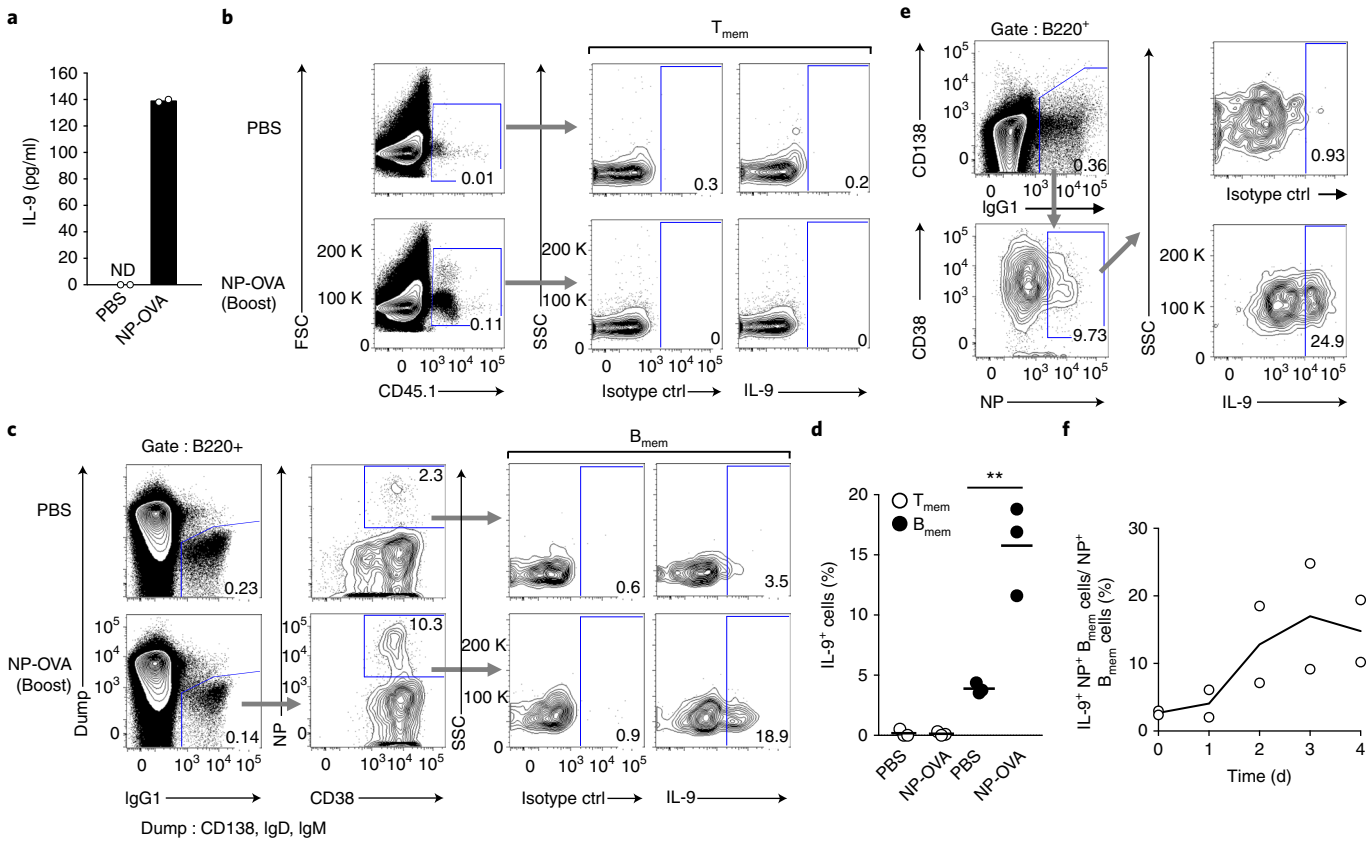

Fig. 7 | B_{mem} cells produce IL-9 during a recall response, but T_{mem} cells do not. a, ELISA of IL-9 in supernatants of cultures of pooled spleen cells from C57BL/6 mice ($n = 3$ per group) given transfer of naive CD4$^+$ OT-II T cells and immunized i.p. with NP-OVA in alum and, 23 weeks later, given intraperitoneal injection of soluble NP-OVA or PBS (horizontal axis) and assessed 3 d later. Each symbol represents an individual replicate ($n = 2$ technical replicates per group); bar tops indicate the mean of the group. **b**,**c**, Flow-cytometry analysis of spleen cells from mice as in **a**, showing intracellular staining (right) of CD45.1$^+$ T_{mem} cells (**b**) or B220$^+$CD138$^-$IgM$^-$IgD$^-$IgG1$^+$NP$^+$CD38$^+$ B_{mem} cells (**c**) (gated as at far left) with monoclonal antibody to IL-9 (IL-9) or isotype-matched control monoclonal antibody (Isotype ctrl). **d**, Frequency of IL-9$^+$ cells among T_{mem} cells or B_{mem} cells (key) as in **b**,**c** (horizontal axis). Each symbol represents an individual mouse ($n = 3$ per group); small horizonal lines indicate the mean. **e**, Flow-cytometry analysis of splenic B220$^+$IgG1$^+$NP$^+$ B_{mem} cells (gated as at left) from C57BL/6 mice immunized i.p. with NP-CGG in alum and, 20 weeks later, with soluble NP-CGG (day 0), assessed by staining of IL-9 (right) as in **c** at 3 d after the rechallenge. **f**, Frequency of IL-9$^+$ cells among the B_{mem} cells in **e**, assessed 1, 2, 3 or 4 d (horizonal axis) after injection of soluble NP-CGG. Each symbol represents an individual mouse ($n = 2$ per time point); line connects mean value at each time point. $^{**}P < 0.01$ (two-tailed unpaired Student's *t*-test). Data are representative of two (**a**,**f**) or three (**b**–**e**) independent experiments with similar results

cells and thus only a small fraction of distantly located GC B cells may begin to express the IL-9R. Such IL-9R$^+$ GC B cells might then undergo differentiation into B_{mem} cells.

IL-9R was clearly expressed on most of IgG1$^+$ B_{mem} cells from 1 week onward. Indeed, ex vivo B_{mem} cells responded to supplementation with IL-9, proliferated and then differentiated into PCs and produced antibodies in vitro. However, a considerable proportion of IgG1$^+$ B_{mem} cells did not seem to express IL-9R at any time point after immunization. The remnant recall response observed in IL-9R-deficient mice might have been caused by such IL-9R$^-$ B_{mem} cells, if they were regulated by (an)other stimulatory receptor(s). Nevertheless, the marked attenuation of the recall response in these mice would suggest that IL-9R$^+$ B_{mem} cells have a major role in recall antibody production, for which IL-9R signaling is essential.

We demonstrated that IL-9 facilitated the CD40-dependent in vitro proliferation and PC differentiation of ex vivo B_{mem} cells, as well as that of IL-9R$^+$ iGB-m cells, in addition to the in vivo defects in the population expansion and antibody production of IL-9R-deficient B_{mem} cells in the recall response. Thus, it seems reasonable to propose that IL-9 signals the proliferation and subsequent PC differentiation of B_{mem} cells after their cognate interaction with memory T cells (T_{mem} cells). In addition, we found that among the B cell surface proteins involved in T cell–B cell interactions and the formation of GCs, ICOSL expression was selectively downregulated by IL-9 in vitro. ICOSL expression on B_{mem} cells is thought to stimulate ICOS on T_{mem} cells, and both ICOSL and ICOS are necessary for GC formation after secondary challenge[40,41]. Thus, IL-9-mediated downregulation of ICOSL expression on B_{mem} cells prevents the T_{mem} cell–mediated development of GC B cells and might further facilitate the PC development of B_{mem} cells during a recall response.

While we were completing this manuscript, another study reported the identification and functional characterization of GC-derived memory precursor cells (GC-MP cells)[33]. In that study, the authors found that IL-9R was expressed on all GC and non-GC B cells and was expressed more abundantly on quiescent (CD38$^+$GL-7$^+$Fas$^+$) GC-MP cells. We confirmed that the GC-MP cells expressed less IL-9R than B_{mem} cells did, but we demonstrated that the bulk of GC (CD38$^-$GL-7$^+$) B cells and follicular B cells expressed little surface IL-9R, if any. The apparent quantitative difference in IL-9R staining might stem from different methods used for staining. The other study used an indirect staining method, with IL-9 plus an IL-9-specific antibody, and with negative controls stained without IL-9[39], whereas we used our original IL-9R-specific monoclonal antibody directly conjugated with

fluorescein to stain B cells from *Il9r*$^{+/+}$ mice and used *Il9r*$^{-/-}$ mice as negative controls.

In addition, the other study demonstrated that abolishing IL-9–IL-9R signaling with a blocking antibody to IL-9 after immunization of mice resulted in a reduction of B_{mem} cells by 30–50%, as assessed at 1–3 weeks after immunization[33]. Similar results were obtained for mice given adoptive transfer of B cells in which IL-9R was knocked down and for bone-marrow chimeras with T cell–restricted IL-9 deficiency[33]. Thus, those authors concluded that IL-9–IL-9R is necessary for the normal development of B_{mem} cells[33]. In our study here, we showed that the number of IgG1$^+$ B_{mem} cells was slightly but not significantly lower in *Il9r*$^{-/-}$ mice than *Il9r*$^{+/+}$ mice and did not decrease more in *Il9r*$^{-/-}$ mice than in *Il9r*$^{+/+}$ mice from 4 weeks to 10 weeks after immunization. Thus, IL-9R signaling did not seem to be required for the gross formation and maintenance of B_{mem} cells. We also showed that *Il9r*$^{-/-}$ B_{mem} cells carried immunoglobulin-encoding genes with somatic hypermutation at a normal mutation frequency and that these genes encoded immunoglobulins with features of increased affinity. The affinity maturation of serum IgG1 during a TD immune response also seemed to be normal in *Il9r*$^{-/-}$ mice. Because the serum titers of antigen-specific IgG1 antibody at a later phase of the primary response in *Il9r*$^{+/+}$ mice were equivalent to those in *Il9r*$^{-/-}$ mice, the production of LLPCs and their maintenance also seemed to be normal in the latter. Therefore, it seems that IL-9–IL-9R signaling is dispensable for B cell differentiation in the later phase of the primary GC response during which SHMs intensively accumulate and most LLPCs are generated[44].

IL-9 was barely detectable in T_{mem} cells responding to antigen but was readily detectable in B_{mem} cells during the recall response. A small proportion of IgG1$^+$ B_{mem} cells remained IL-9$^+$ for months after the primary immunization, and the proportion of the IL-9$^+$ IgG1$^+$ B_{mem} cells rapidly increased to ~20% after the secondary immunization. Indeed, IL-9 was detectable in culture supernatants of B_{mem} cells directly ex vivo, although its concentration was apparently not enough for in vitro auto-activation. If B_{mem} cells proliferate as aggregates in situ after encountering antigen and cognate T_{mem} cells, the local concentration of the B_{mem} cell–derived IL-9 might be sufficient for auto-activation, which could exponentially accelerate the recall response. Autocrine and/or paracrine stimulation through IL-9 and IL-9R probably directs the proliferation of IL-9R$^+$ B_{mem} cells and commits them to development into PCs while suppressing GC formation through IL-9R-mediated downregulation of ICOSL expression in the recall response. If so, modulation of IL-9–IL-9R signaling during repeated immunization with vaccines should make it possible to control the outcome of the immunization; for example, by inhibition of IL-9–IL-9R signaling to suppress antibody production while facilitating the further affinity maturation and maintenance of B_{mem} cells or by hyper-stimulation to augment antibody production.

Methods

Methods, including statements of data availability and any associated accession codes and references, are available at https://doi.org/10.1038/s41590-018-0177-0.

Received: 9 September 2017; Accepted: 8 June 2018;
Published online: 6 August 2018

References

1. McHeyzer-Williams, M., Okitsu, S., Wang, N. & McHeyzer-Williams, L. Molecular programming of B cell memory. *Nat. Rev. Immunol.* **12**, 24–34 (2011).
2. Shlomchik, M. J. & Weisel, F. Germinal center selection and the development of memory B and plasma cells. *Immunol. Rev.* **247**, 52–63 (2012).
3. Chan, T. D. & Brink, R. Affinity-based selection and the germinal center response. *Immunol. Rev.* **247**, 11–23 (2012).
4. Suan, D., Sundling, C. & Brink, R. Plasma cell and memory B cell differentiation from the germinal center. *Curr. Opin. Immunol.* **45**, 97–102 (2017).
5. Ise, W. et al. Memory B cells contribute to rapid Bcl6 expression by memory follicular helper Tcells. *Proc. Natl. Acad. Sci. USA* **111**, 11792–11797 (2014).
6. Crotty, S. The 1-1-1 fallacy. *Immunol. Rev.* **247**, 133–142 (2012).
7. Schaerli, P. et al. CXC chemokine receptor 5 expression defines follicular homing T cells with B cell helper function. *J. Exp. Med.* **192**, 1553–1562 (2000).
8. Kim, C. H. et al. Subspecialization of CXCR5$^+$ T cells: B helper activity is focused in a germinal center-localized subset of CXCR5$^+$ T cells. *J. Exp. Med.* **193**, 1373–1381 (2001).
9. Linterman, M. A. et al. IL-21 acts directly on B cells to regulate Bcl-6 expression and germinal center responses. *J. Exp. Med.* **207**, 353–363 (2010).
10. Ozaki, K. et al. A critical role for IL-21 in regulating immunoglobulin production. *Science* **298**, 1630–1634 (2002).
11. Bessa, J., Kopf, M. & Bachmann, M. F. Cutting edge: IL-21 and TLR signaling regulate germinal center responses in a B cell-intrinsic manner. *J. Immunol.* **184**, 4615–4619 (2010).
12. Rasheed, M. A. et al. Interleukin-21 is a critical cytokine for the generation of virus-specific long-lived plasma cells. *J. Virol.* **87**, 7737–7746 (2013).
13. Zotos, D. et al. IL-21 regulates germinal center B cell differentiation and proliferation through a B cell-intrinsic mechanism. *J. Exp. Med.* **207**, 365–378 (2010).
14. Rankin, A. L. et al. IL-21 receptor is critical for the development of memory B cell responses. *J. Immunol.* **186**, 667–674 (2011).
15. McGuire, H. M. et al. IL-21 and IL-4 collaborate to shape T-dependent antibody responses. *J. Immunol.* **195**, 5123–5135 (2015).
16. Harada, Y. et al. The 3′ enhancer CNS2 is a critical regulator of interleukin-4-mediated humoral immunity in follicular helper T cells. *Immunity* **36**, 188–200 (2012).
17. Reinhardt, R. L., Liang, H. E. & Locksley, R. M. Cytokine-secreting follicular T cells shape the antibody repertoire. *Nat. Immunol.* **10**, 385–393 (2009).
18. Vijayanand, P. et al. Interleukin-4 production by follicular helper T cells requires the conserved Il4 enhancer hypersensitivity site V. *Immunity* **36**, 175–187 (2012).
19. Yu, A. et al. Efficient induction of primary and secondary T cell-dependent immune responses in vivo in the absence of functional IL-2 and IL-15 receptors. *J. Immunol.* **170**, 236–242 (2003).
20. Wilhelm, C. et al. An IL-9 fate reporter demonstrates the induction of an innate IL-9 response in lung inflammation. *Nat. Immunol.* **12**, 1071–1077 (2011).
21. Noelle, R. J. & Nowak, E. C. Cellular sources and immune functions of interleukin-9. *Nat. Rev. Immunol.* **10**, 683–687 (2010).
22. Stassen, M. et al. Murine bone marrow-derived mast cells as potent producers of IL-9: costimulatory function of IL-10 and kit ligand in the presence of IL-1. *J. Immunol.* **164**, 5549–5555 (2000).
23. Licona-Limón, P. et al. Th9 Cells drive host immunity against gastrointestinal worm infection. *Immunity* **39**, 744–757 (2013).
24. Gounni, A. S. et al. IL-9 expression by human eosinophils: regulation by IL-1β and TNF-α. *J. Allergy Clin. Immunol.* **106**, 460–466 (2000).
25. Renauld, J. C. et al. Expression cloning of the murine and human interleukin 9 receptor cDNAs. *Proc. Natl. Acad. Sci. USA* **89**, 5690–5694 (1992).
26. Bauer, J. H., Liu, K. D., You, Y., Lai, S. Y. & Goldsmith, M. A. Heteromerization of the γc chain with the interleukin-9 receptor α subunit leads to STAT activation and prevention of apoptosis. *J. Biol. Chem.* **273**, 9255–9260 (1998).
27. Kaplan, M. H., Hufford, M. M. & Olson, M. R. The development and in vivo function of T helper 9 cells. *Nat. Rev. Immunol.* **15**, 295–307 (2015).
28. Petit-Frere, C., Dugas, B., Braquet, P. & Mencia-Huerta, J. M. Interleukin-9 potentiates the interleukin-4-induced IgE and IgG1 release from murine B lymphocytes. *Immunology* **79**, 146–151 (1993).
29. Dugas, B. et al. Interleukin-9 potentiates the interleukin-4-induced immunoglobulin (IgG, IgM and IgE) production by normal human B lymphocytes. *Eur. J. Immunol.* **23**, 1687–1692 (1993).
30. Vink, A., Warnier, G., Brombacher, F. & Renauld, J. C. Interleukin 9-induced in vivo expansion of the B-1 lymphocyte population. *J. Exp. Med.* **189**, 1413–1423 (1999).
31. Nojima, T. et al. In-vitro derived germinal centre B cells differentially generate memory B or plasma cells in vivo. *Nat. Commun.* **2**, 465 (2011).
32. Steenwinckel, V. et al. IL-13 mediates in vivo IL-9 activities on lung epithelial cells but not on hematopoietic cells. *J. Immunol.* **178**, 3244–3251 (2007).
33. Wang, Y. et al. Germinal-center development of memory B cells driven by IL-9 from follicular helper T cells. *Nat. Immunol.* **18**, 921–930 (2017).

34. Fawaz, L. M. et al. Expression of IL-9 receptor α chain on human germinal center B cells modulates IgE secretion. *J. Allergy Clin. Immunol.* **120**, 1208–1215 (2007).
35. Kocks, C. & Rajewsky, K. Stepwise intraclonal maturation of antibody affinity through somatic hypermutation. *Proc. Natl. Acad. Sci. USA* **85**, 8206–8210 (1988).
36. Taylor, J. J., Pape, K. A. & Jenkins, M. K. A germinal center-independent pathway generates unswitched memory B cells early in the primary response. *J. Exp. Med.* **209**, 597–606 (2012).
37. Zuccarino-Catania, G. V. et al. CD80 and PD-L2 define functionally distinct memory B cell subsets that are independent of antibody isotype. *Nat. Immunol.* **15**, 631–637 (2014).
38. Tomayko, M. M., Steinel, N. C., Anderson, S. M. & Shlomchik, M. J. Cutting edge: hierarchy of maturity of murine memory B cell subsets. *J. Immunol.* **185**, 7146–7150 (2010).
39. He, J. S. et al. IgG1 memory B cells keep the memory of IgE responses. *Nat. Commun.* **8**, 641 (2017).
40. Dong, C., Temann, U. A. & Flavell, R. A. Cutting edge: critical role of inducible costimulator in germinal center reactions. *J. Immunol.* **166**, 3659–3662 (2001).
41. Wong, S. C., Oh, E., Ng, C. H. & Lam, K. P. Impaired germinal center formation and recall T-cell-dependent immune responses in mice lacking the costimulatory ligand B7-H2. *Blood* **102**, 1381–1388 (2003).
42. Yoshinaga, S. K. et al. T-cell co-stimulation through B7RP-1 and ICOS. *Nature* **402**, 827–832 (1999).
43. Swallow, M. M., Wallin, J. J. & Sha, W. C. B7h, a novel costimulatory homolog of B7.1 and B7.2, is induced by TNFα. *Immunity* **11**, 423–432 (1999).
44. Weisel, F. J., Zuccarino-Catania, G. V., Chikina, M. & Shlomchik, M. J. A temporal switch in the germinal center determines differential output of memory B and plasma Cells. *Immunity* **44**, 116–130 (2016).

Acknowledgements

We thank A. Ainai and H. Hasegawa (National Institute of Infectious Diseases) for the vaccine containing whole inactivated influenza virus; S. Horiuchi, T. Koike, T. Katayama, I. Shiratori and Y. Takai for reagents and technical assistance; other members of the Research Institute for Biomedical Sciences for technical advice and comments; Y. Takatsuka for figure preparation; and P. Burrows for critical reading. This work was supported by the Japan Society for the Promotion of Science KAKENHI, Grant-in-Aid for Scientific Research (B) (16H05206) and Grant-in-Aid for Scientific Research on Innovative Areas (25111512) (all to D.K.).

Author contributions

S.T. designed and performed experiments, analyzed data and wrote the manuscript; H.Y., K.H., H.S. and M.I. performed experiments and analyzed data; J.-C.R. made the IL-9R-deficient mice; and D.K. supervised the study, designed experiments and wrote the manuscript.

Competing interests

The authors declare no competing interests.

Additional information

Supplementary information is available for this paper at https://doi.org/10.1038/s41590-018-0177-0.

Reprints and permissions information is available at www.nature.com/reprints.

Correspondence and requests for materials should be addressed to D.K.

Publisher's note: Springer Nature remains neutral with regard to jurisdictional claims in published maps and institutional affiliations.

Methods

Mice and immunization. C57BL/6NCrSlc (B6; CD45.2$^+$) mice were purchased from Sankyo Lab Service. *Il9r*$^{-/-}$ mice[30], B1-8ki mice[45] and μMT mice[46] were backcrossed to the B6 strain. OT-II mice[47] on the B6 background and congenic B6 CD45.1$^+$ strains were intercrossed to generate OT-II CD45.1$^+$CD45.2$^+$ F_1 mice. Mice were immunized i.p. with 100 μg $NP_{30\text{-}40}$–CGG (30–40 molecules of NP (4-hydroxy-3-nitrophenyl)acetyl) conjugated to CGG) precipitated in alum and were boosted i.v. with 25 μg soluble $NP_{30\text{-}40}$–CGG unless otherwise noted. In ICOSL-blocking studies, immunized mice were given intravenous injection of ICOSL-specific monoclonal antibody (mAb) (HK5.3, BE0028, BioXCell; 200 μg per mouse) or isotype-matched control mAb (2A3, BE0089, BioXCell; 200 μg/mouse) 1 d before and 3 d after secondary immunization with soluble antigen. Mice were inoculated subcutaneously with formalin-inactivated whole influenza A virus, A/Puerto Rico/8/34, H1N1 (PR8)[48] and were rechallenged i.v. (1 μg total protein per mouse). All animals were maintained in a mouse facility in Research Institute for Biomedical Sciences, Tokyo University of Science under specific pathogen-free conditions and were treated under protocols approved by the Animal Care and Use Committee of the Tokyo University of Science.

Generation of IL-9R-specific mAbs. Female Lew/SSN rats (Sankyo Lab Service) were used for immunization with DNA. Intramuscular injection of plasmid followed by in vivo electroporation were performed as previously described for mice[49] with the following modifications. In brief, 30 μl (10 mg/ml) of pCADEST1 carrying a gene encoding IL-9R–GroEL fusion protein was injected into the quadriceps muscles that had been given injection of 100 μl (1 U/ μl) of bovine hyaluronidase 10 min earlier, by using a syringe fitted with a two-stage needle (26 gauge). The same DNA immunization protocol was repeated 1, 3, 4, 7 and 9 weeks after the primary immunization. At 27 weeks after the primary immunization, the rat showing the highest titer of IL-9R-specific antibody after the final immunization was given intraperitoneal transfer of 1×10^9 irradiated (30 Gy) B300-19 mouse pre-B cells stably expressing IL-9R (B300-19–IL-9R). Then, 3 d later, hybridomas were generated by a conventional method using SP2/0 myeloma as the fusion partner. B300-19–IL-9R cells were generated by transduction of B300-19 cells with a retroviral vector containing *Il9r* cDNA (pMXs-IL9R-IRES-hNGFR), as described previously[50].

Generation of bone marrow chimeras. Bone marrow cells from at least three *Il9r*$^{+/+}$ or *Il9r*$^{-/-}$mice and μMT mice, mixed at 1:4, were injected i.v. (4×10^6 cells per mouse) into lethally irradiated C57BL/6 mice (5.5 Gy, twice at 3-hour intervals). The resultant chimeras were used for immunization at least 7–8 weeks after the transfer.

Adoptive transfer. To analyze recall response of B_{mem} cells, B cells including the same number of B_{mem} cells of pooled spleens of *Il9r*$^{+/+}$ or *Il9r*$^{-/-}$mice (six per group) immunized with NP-CGG in alum 7 weeks earlier, and pooled spleen cells from five C57BL/6 mice primed with CGG in alum 2 weeks earlier, were co-transferred i.v. into C57BL/6 mice. To detect IgM$^+$ B_{mem} cells, B cells purified from CD45.1$^+$ B1-8ki *Il9r*$^{+/+}$ or *Il9r*$^{-/-}$ mice were labeled with CFSE (carboxyfluorescein diacetate succinimidyl ester) as previously described[36] and were transferred i.v. into B6 mice. To induce anti-OVA T_{mem} cells, naive CD4$^+$ T cells purified from OT-II CD45.1$^+$CD45.2$^+$ F_1 mice were transferred i.v. into B6 mice.

Quantitative real-time PCR. RNA preparation, cDNA synthesis and quantitative real-time PCR (qRT-PCR) were performed, and data are presented as described previously[31]. Gene expression was normalized to that of the control gene *Gapdh*. The following primer sets were used:

Gapdh sense: 5′-GGAGAAACCTGCCAAGTATGA-3′;
Gapdh antisense: 5′-CCCTGTTGCTGTAGCCGTATT-3′;
Il9r sense: 5′- GGACAGTTGGCAGTAAGTCACC-3′;
Il9r antisense: 5′ -CCACTCTCTCCAAGGTCCAA-3′;
Prdm1 sense: 5′-ACGTGTGGGTACGACCTTG-3′;
Prdm1 antisense: 5′-CCATGTCCATTTTCATGATCC-3′;
Icosl sense: 5′- CGCACATGCAGCTAAAGT-3′;
Icosl antisense: 5′-AAACATGGAGCTTCTTCCAAAC-3′;

Cell purification and culture. B cells were cultured, in a humidified atmosphere at 37 °C with 5% CO_2, in the following 'B cell medium' (BCM): RPMI-1640 medium (Wako) supplemented with 10% heat-inactivated FBS (FBS), 1 mM sodium pyruvate, 50 μM 2-mercaptoethanol, 10 mM HEPES pH7.5, 100 U/ml penicillin and 100 μg/ml streptomycin (GIBCO). Naive B cell purification was performed as described[31]. For analysis of the expression of *Il9r* mRNA or IL-9R, follicular B cells (AA4.1$^-$ B220$^+$ IgM$^+$ CD23^{hi}), marginal-zone B cell (AA4.1$^-$ B220$^+$ IgM$^+$ CD23^{lo}), GC B cells (B220$^+$ IgG1$^+$ NP$^+$ CD38^{lo}) and B_{mem} cells (B220$^+$ IgG1$^+$ NP$^+$ CD38^{hi}) were sorted from pooled spleen cells of at least five unimmunized C57BL/6 mice (follicular B cells and marginal-zone B cells) or those immunized with NP-CGG in alum 8 d earlier (GC B cells) or 28 d earlier (B_{mem} cells), using a FACSAria II (BD Biosciences). In other experiments, B_{mem} cells were purified from mice immunized i.p. with NP-CGG and alum at least 6 weeks earlier: pooled splenocytes from 20 mice were stained with biotin anti-CD4, anti-CD8, anti-DX5, anti-Gr-1, anti-TER-119 and anti-CD43(S7), with avidin-particle-DM (BD Biosciences), and then positive cells were depleted using the MACS system (Miltenyi Biotec). From the remaining cells, B_{mem} cells (B220$^+$ NP$^+$ IgG1$^+$CD38$^+$) were sorted using a FACSAria II. These procedures yielded 95% purity B_{mem} cells. Naive CD4$^+$ T cells (CD4$^+$CD3ε$^+$CD62L^{hi}) were purified, with the MACS system and a FACSAria II, from splenocytes stained with biotinylated mAbs to CD4, CD3ε and CD62L as shown in Supplementary Fig. 6c . For in vitro stimulation, purified B cells were cultured with lipopolysaccharide (10 μg/ml), anti-IgM (10 μg/ml), anti-CD40 (10 μg/ml), IL-4 (10 ng/ml), IL-21 (10 ng/ml), or IL-9 (1 ng/ml), alone or in the indicated combination, in BCM at 37 °C in a 5% CO_2 incubator. T_H9 cells were generated as previously reported[51] with a minor modification: splenocytes were cultured with anti-CD28 (37.51: 5 μg/ml), TGF-β1 (10 ng/ml), IL-4 (10 ng/ml), IL-2 (20 ng/ml), anti-IFN-γ (10 μg/ml), and plate-coated anti-CD3ε (145-2C11) for 3 d in BCM. Reagents are identified (including clone or catalog number and vendor for antibodies) in Supplementary Table 1.

iGB cell culture. iGB cell culture[31] and retroviral transduction[50] were performed as previously described with the following modifications unless otherwise noted: naive B and B_{mem} cells were cultured on 40LB feeder cells for 3 d for the primary and the secondary culture and for 2 d for the tertiary culture, with or without the indicated cytokines. IL-4 (10 ng/ml), IL-21 (10 ng/ml), or IL-9 (1 ng/ml) was added in the culture medium where indicated. The 40LB cell line used in this study is a subline of original 40LB cells[31], selected to express CD40L more abundantly than the original 40LB cells by repeated transduction with a CD40L-expressing retrovirus.

Flow cytometry. Single-cell suspensions from spleens were depleted of RBCs by ammonium chloride lysis, incubated with mAb to FcγRII/III (2.4G2; BD Pharmingen) to block FcγRs and were stained for 30 min on ice in PBS containing 0.5% BSA, 2 mM EDTA, 0.05% sodium azide with various combinations of antibodies and reagents (Supplementary Table 1). IL-9R was detected with a fusion protein of mouse IL-9 and human IgG1 Fc (IL-9–Fc) and Alexa Fluor 647-conjugated goat anti–human IgG (Supplementary Table 1) or with Alexa Fluor 647-conjugated rat mAbs to mouse IL-9R (RZ-66, RZ-87, RZ-98 and RZ-103) generated in-house as described above. To stain intracellular IL-9, cells were incubated with 2 μM of monensin for 5 h at 37 °C and then were treated with Cytofix/Cytoperm solution and Perm/Wash buffer (BD Biosciences) according to the manufacturer's protocol before being staines with mAb to IL-9 (50-8091-80; eBiosciences) or isotype-matched control mAb (50-4301-80; eBioscience). All samples were analyzed using a FACSCalibur or FACSCanto II (BD Biosciences). The data were analyzed using FlowJo (Tree Star).

ELISA. NP-specific IgG1, IgG2b, IgG2c, IgG3, IgM and hemagglutinin-specific IgG were detected by ELISA as described previously[52,53]. IL-9 was detected in the supernatants of spleen cells (5×10^7 cells per well of 6-well plate) or B_{mem} cells (Supplementary Fig. 7c), cultured for 3 or 6 d, respectively, using an ELISA kit (eBioscience, cat#88-8092-22).

B_{mem} cell sorting and V_H sequence analysis. B_{mem} cells were magnetically enriched from pooled spleens using biotinylated anti-CD43, anti-Ter119, anti-CD4, anti-CD8, anti-CD49b, anti-IgD and streptavidin particle DM (antibody identification, Supplementary Table 1) in combination with iMag (BD) and MACS system (Miltenyi). Enriched cells were stained with fluorochrome conjugated anti-B220, anti–immunoglobulin κ-chain, anti-IgG1, anti-CD38 and Alexa 647 conjugated NP-BSA (antibody identification, Supplementary Table 1), and then NP-specific IgG1$^+$ B_{mem} cells were sorted, using a FACSAria II (BD Biosciences), directly into KOD Fx Neo buffer (Toyobo) containing 0.1 mg/ml proteinase K (Merck). Samples were incubated at 55 °C for 1 h followed by 95 °C for 10 min, and then mixture of KOD Fx Neo buffer, dNTPs (Toyobo), primers and KOD DNA polymerase (Toyobo) were added. To amplify V_H186.2 sequences, nested PCR was performed as described previously[50]. Amplified fragments were cloned into pBluescript II vector (Invitrogen) and sequenced (Eurofins Genomics).

In vitro cell-survival analysis. NP-binding IgG1$^+$ GC B cells (CD19$^+$ CD38^{lo} GL-7$^+$) and B_{mem} cells (CD19$^+$ CD38^{hi} GL-7$^-$) were purified from pooled splenocytes of B6 mice that had been immunized with NP-CGG, and naive B cells (CD19$^+$ IgD$^+$ CD38^{hi}) were purified from an unimmunized B6 mouse, through iMag (BD), MACS (Miltenyi) and a FACSAria II (BD). Sorted cells were cultured with or without IL-9 (1 ng/ml) in BCM for 12 or 24 h in 96-well plates (1×10^3 cells per well) in vitro. These cells were then stained with propidium iodide and analyzed by flow cytometry.

Statistical analysis. Statistical analysis was performed using the two-tailed unpaired Student *t*-test, non-parametric Mann–Whitney test, or one- or two-way analysis of variance (ANOVA) with Tukey's multiple comparison tests (one- or two-way ANOVA) by using Prizm software where indicated.

Reporting Summary. Further information on experimental design is available in the Nature Research Reporting Summary linked to this article.

Data availability statement. The data that support the findings of this study are available from the corresponding author upon request.

References

45. Kitamura, D., Roes, J., Kuhn, R. & Rajewsky, K. A B cell-deficient mouse by targeted disruption of the membrane exon of the immunoglobulin μ chain gene. *Nature* **350**, 423–426 (1991).
46. Lam, K. P., Kühn, R. & Rajewsky, K. In vivo ablation of surface immunoglobulin on mature B cells by inducible gene targeting results in rapid cell death. *Cell* **90**, 1073–1083 (1997).
47. Barnden, M. J., Allison, J., Heath, W. R. & Carbone, F. R. Defective TCR expression in transgenic mice constructed using cDNA-based alpha- and beta-chain genes under the control of heterologous regulatory elements. *Immunol. Cell Biol.* **76**, 34–40 (1998).
48. Tamura, S. et al. Cross-protection against influenza virus infection afforded by trivalent inactivated vaccines inoculated intranasally with cholera toxin B subunit. *J. Immunol.* **149**, 981–988 (1992).
49. Takatsuka, S., Sekiguchi, A., Tokunaga, M., Fujimoto, A. & Chiba, J. Generation of a panel of monoclonal antibodies against atypical chemokine receptor CCX-CKR by DNA immunization. *J. Pharmacol. Toxicol. Methods* **63**, 250–257 (2011).
50. Haniuda, K., Fukao, S., Kodama, T., Hasegawa, H. & Kitamura, D. Autonomous membrane IgE signaling prevents IgE-memory formation. *Nat. Immunol.* **17**, 1109–1117 (2016).
51. Végran, F. et al. The transcription factor IRF1 dictates the IL-21-dependent anticancer functions of T_H9 cells. *Nat. Immunol.* **15**, 758–766 (2014).
52. Haniuda, K., Nojima, T., Ohyama, K. & Kitamura, D. Tolerance induction of IgG^+ memory B cells by T cell-independent type II antigens. *J. Immunol.* **186**, 5620–5628 (2011).
53. Ainai, A. et al. Zymosan enhances the mucosal adjuvant activity of poly(I:C) in a nasal influenza vaccine. *J. Med. Virol.* **82**, 476–484 (2010).

nature research

Corresponding author(s): Daisuke Kitamura

☐ Initial submission ☐ Revised version ☒ Final submission

Life Sciences Reporting Summary

Nature Research wishes to improve the reproducibility of the work that we publish. This form is intended for publication with all accepted life science papers and provides structure for consistency and transparency in reporting. Every life science submission will use this form; some list items might not apply to an individual manuscript, but all fields must be completed for clarity.

For further information on the points included in this form, see Reporting Life Sciences Research. For further information on Nature Research policies, including our data availability policy, see Authors & Referees and the Editorial Policy Checklist.

Experimental design

1. Sample size

Describe how sample size was determined.

Generally accepted sample sizes were used. Sample size was determined according to standard practices and to our previous experience. Sample size and associated statistics are indicated in the figure legend.

2. Data exclusions

Describe any data exclusions.

No data were excluded from the analyses except those from preliminary experiments, i.e. the first trial with n = 1 biological samples.

3. Replication

Describe whether the experimental findings were reliably reproduced.

Experimental findings were reliably reproduced.

4. Randomization

Describe how samples/organisms/participants were allocated into experimental groups.

Mice with the same genotype, the same sex, and the similar age, were randomly selected into each experimental group.

5. Blinding

Describe whether the investigators were blinded to group allocation during data collection and/or analysis.

Investigators were not blinded to group allocation during data collection and analyses, because usually one investigator sets up experimental groups as above, performs the experiment, and analyzes data in one experiment, and therefore it is almost impossible to be blinded to group allocation.

Note: all studies involving animals and/or human research participants must disclose whether blinding and randomization were used.

6. Statistical parameters

For all figures and tables that use statistical methods, confirm that the following items are present in relevant figure legends (or in the Methods section if additional space is needed).

n/a	Confirmed
☐	☒ The exact sample size (*n*) for each experimental group/condition, given as a discrete number and unit of measurement (animals, litters, cultures, etc.)
☐	☒ A description of how samples were collected, noting whether measurements were taken from distinct samples or whether the same sample was measured repeatedly
☐	☒ A statement indicating how many times each experiment was replicated
☐	☒ The statistical test(s) used and whether they are one- or two-sided (note: only common tests should be described solely by name; more complex techniques should be described in the Methods section)
☐	☒ A description of any assumptions or corrections, such as an adjustment for multiple comparisons
☐	☒ The test results (e.g. *P* values) given as exact values whenever possible and with confidence intervals noted
☐	☒ A clear description of statistics including central tendency (e.g. median, mean) and variation (e.g. standard deviation, interquartile range)
☐	☒ Clearly defined error bars

See the web collection on statistics for biologists for further resources and guidance.

Software

Policy information about availability of computer code

7. Software

Describe the software used to analyze the data in this study.	FlowJo, MPM6, Excel, GraphPad Prism 7

For manuscripts utilizing custom algorithms or software that are central to the paper but not yet described in the published literature, software must be made available to editors and reviewers upon request. We strongly encourage code deposition in a community repository (e.g. GitHub). *Nature Methods* guidance for providing algorithms and software for publication provides further information on this topic.

Materials and reagents

Policy information about availability of materials

8. Materials availability

Indicate whether there are restrictions on availability of unique materials or if these materials are only available for distribution by a for-profit company.	40LB or anti-IL-9R monoclonal antibodies generated by us will be available upon request.

9. Antibodies

Describe the antibodies used and how they were validated for use in the system under study (i.e. assay and species).	Antibodies used in this study were either previously validated by other researchers or by the companies where we purchased. Anti-IL-9R antibodies (in-house) were validated by comparison of the staining of cells from Il9r+/+ and -/- mice by flow cytometry. Antibodies used in this work are listed below: Anti-ICOSL clone HK5.3, Thermo, #12-5985-81 (FCM_1:250) Anti-IgD clone 11-26c.2a, Biolegend, #405733, 405705, 405709 (FCM_1:250) Anti-IgE clone RME-1, Biolegend, #406903, 406905, 406907 (FCM_1:500dil) Anti-IgM clone II/41, Thermo, #13-5790-81, 12-5790-81 (FCM_1:250) Anti-IgG1 clone A85-1, BD, #562580, 562026, 560089 (FCM_1:500-1000dil) Anti-IL-9 clone RM9A4, Thermo, #50-8091-80 (FCM_1:167dil) Anti-IL-9R clone RZ-66, -87, -98, -103, (In house), - (FCM_1:250) Anti-IL-21R clone 4A9, Biolegend, #131909 (FCM_1:500-1000dil) Anti-I-A/I-E (MHCII) clone M5/114.15.2, Biolegend, #107605 (FCM_1:1000dil) Anti-CD3ε clone 145-2C11, Biolegend, #100305 (FCM_1:250) Anti-CD4 clone RM4-5, Biolegend, #100509, 100511, 100515, 100543 (FCM_1:500dil) Anti-CD11b clone M1/70, Biolegend, #101211, 101223 (FCM_1:500dil) Anti-CD11c clone N418, Biolegend, #117305, 117307 (FCM_1:500dil) Anti-CD38 clone 90, Thermo, #A15393, 12-0381-81, 25-0381-80 (FCM_1:500-1000dil) Anti-CD40 clone 1C10, Thermo, #12-0401-81 (FCM_1:250) Anti-CD45.1 clone A20, Biolegend, #110705, 110713, 110715, 110731 (FCM_1:250) Anti-CD45.2 clone 104, Biolegend, #109805, 109807, 109813 (FCM_1:250) Anti-CD45R/B220 clone RA3-6B2, Biolegend, #103211, 103221, 103223 (FCM_1:250) Anti-CD62L clone MEL-14, Biolegend, #104403, 104411 (FCM_1:500dil) Anti-CD80 clone 16-10A1, Biolegend, #104705, 104707 (FCM_1:500dil) Anti-CD138 clone 281-2, Biolegend, #142511, 142507, 142503 (FCM_1:500dil) Anti-CD271 (NGFR) clone ME20.4, Biolegend, #345107, 345109 (FCM_1:250) Anti-CD275 (ICOSL) clone HK5.3, Thermo, #12-5985-81 (FCM_1:250) Anti-CXCR5 clone 2G8, BD, #551960 (FCM_1:250) Anti-c-kit clone 2B8, Thermo, #17-1171-81 (FCM_1:250) Anti-FcεRIα clone MAR-1, Biolegend, #134315 (FCM_1:250) Anti-F4/80 clone BM8, Biolegend, #123107, 123109 (FCM_1:250) Anti-Ly6C clone HK1.4, Biolegend, #128021 (FCM_1:1000dil) Anti-NK1.1 clone PK136, Thermo, #13-5941-81, 12-5941-81 (FCM_1:250) Anti-PD1 clone J43, Thermo, #25-9985-80 (FCM_1:500dil) Anti-PD-L2 clone TY25, Thermo, #11-9972-81, 13-5986-81 (FCM_1:250) rat IgG1 isotype contorol clone eBRG1, Thermo, #50-4301-80 (FCM_1:167dil) Anti-STAT3 (pY705) clone 4/P-STAT3, BD, #562072 (FCM_1:5dil) Anti-STAT5 (pY694) clone 47/Stat5(pY694), BD, #562076 (FCM_1:5dil) Anti-Siglec F clone E50-2440, BD, #562068 (FCM_1:250) Anti-TCRβ clone H57-597, Biolegend, #109205 (FCM_1:250) Anti-T- and B- Cell activation antigen clone GL-7, BD, #562080 (FCM_1:500dil) Anti-T- and B- Cell activation antigen clone GL-7, Biolegend, #144609 (FCM_1:500dil) Anti-Gr-1 clone RB-6-8C5, Biolegend, #108403 (FCM, Purification_1:1000dil) Anti-H-2Kd clone SF1-1.1, Biolegend, #116617, 116603 (FCM, Purification_1:500dil)

10. Eukaryotic cell lines

a. State the source of each eukaryotic cell line used.

Balb/c 3T3 cell line was provided by RIKEN BioResource Center.

b. Describe the method of cell line authentication used.

We obtained Balb/c 3T3 cell line directly from RIKEN BioResource Center and therefore have not further authenticated.

c. Report whether the cell lines were tested for mycoplasma contamination.

All cell lines were tested and were negative for mycoplasma contamination.

d. If any of the cell lines used are listed in the database of commonly misidentified cell lines maintained by ICLAC, provide a scientific rationale for their use.

No commonly misidentified cell lines were used.

Animals and human research participants

Policy information about studies involving animals; when reporting animal research, follow the ARRIVE guidelines

11. Description of research animals

Provide details on animals and/or animal-derived materials used in the study.

C57BL/6NCrSlc (B6; CD45.2) mice were purchased from Sankyo Lab Service. Il9r–/– mice, B1-8ki mice and μMT mice were backcrossed to the B6 strain. OT-II transgenic mice (OT-II) of B6 background and congenic B6-CD45.1 strains were intercrossed to generate OT-II CD45.1/CD45.2 F1 mice. Male and female mice were used at 6-10 weeks of age. Female Lew/SSN rats were purchased from Sankyo Lab Service. Rats were used at 4 weeks of age.

Policy information about studies involving human research participants

12. Description of human research participants

Describe the covariate-relevant population characteristics of the human research participants.

This study did not involve human research participants.